IMA Journal of Numerical Analysis (2017) **37**, 2004–2019
doi: 10.1093/imanum/drw049
Advance Access publication on September 29, 2016

An adaptive space-time Newton–Galerkin approach for semilinear singularly perturbed parabolic evolution equations

MARIO AMREIN AND THOMAS P. WIHLER*
Mathematics Institute, University of Bern, CH-3012 Bern, Switzerland
*Corresponding author: mario.amrein@hslu.ch wihler@math.unibe.ch

[Received on 15 January 2016; revised on 17 August 2016]

In this article, we develop an adaptive procedure for the numerical solution of semilinear parabolic problems with possible singular perturbations. Our approach combines a linearization technique using Newton's method with an adaptive discretization—which is based on a spatial finite element method and the backward Euler time-stepping scheme—of the resulting sequence of linear problems. Upon deriving a robust *a posteriori* error analysis, we design a fully adaptive Newton–Galerkin time-stepping algorithm. Numerical experiments underline the robustness and reliability of the proposed approach for various examples.

Keywords: Newton methods; semilinear parabolic problems; singularly perturbed problems; adaptive space-time discretizations.

1. Introduction

Semilinear evolution problems appear in a wide range of applications including, for instance, ecology, (bio)chemistry, quantum physics, astrophysics, material science and optics; see Chandrasekhar (1939), Kelley (1965), Jäger & Luckhaus (1992), Barles & Burdeau (1995), Okubo & Levin (2001), Cantrell & Cosner (2003), Borisyuk *et al.* (2005), Edelstein-Keshet (2005), Barles & Perthame (2007) and Perthame (2007). In this contribution, we consider the numerical approximation of semilinear parabolic equations with a possibly degenerate diffusion coefficient $0 < \varepsilon \ll 1$. Specifically, for a continuously differentiable nonlinearity $f : \mathbb{R} \times \Omega \times (0, T] \to \mathbb{R}$, and an initial function $g \in L^2(\Omega)$, we study initial/boundary value problems of the form

$$\begin{aligned} \partial_t u(\boldsymbol{x}, t) - \varepsilon \Delta u(\boldsymbol{x}, t) &= f(u(\boldsymbol{x}, t), \boldsymbol{x}, t), && (\boldsymbol{x}, t) \in \Omega \times (0, T], \\ u(\boldsymbol{x}, t) &= 0, && (\boldsymbol{x}, t) \in \partial\Omega \times (0, T], \\ u(\boldsymbol{x}, 0) &= g(\boldsymbol{x}), && \boldsymbol{x} \in \Omega. \end{aligned} \tag{1.1}$$

Here $\Omega \subset \mathbb{R}^d$, with $d \in \{1, 2\}$, is an open and bounded one-dimensional interval or a two-dimensional Lipschitz polygon, respectively. Furthermore, $T \in (0, \infty)$ denotes the final time of the evolutionary process. In the singularly perturbed case, $\varepsilon \ll 1$, solutions of (1.1) are known to exhibit boundary layers, interior shocks or (multiple) spikes. The numerical solution of (1.1) in the presence of such singular effects is challenging (see, e.g., Verhulst, 2005; Roos *et al.*, 2008), and requires carefully selected discretizations of the time and space variables. In particular, the proper resolution of layers and spikes (or even of blow-up areas) mandates the use of *adaptive* refinements of the underlying discrete spaces. Indeed, standard numerical methods based on fixed discretizations may possibly fail to recover the true solution behaviour of (1.1); cf., e.g., Stuart & Floater (1990). We note that this might happen even if the nonlinear systems resulting from the discretizations are accurately treated by means of a nonlinear solver. This motivates

us to develop an approach, to be outlined in the sequel, by which the temporal and spatial discretization errors, as well as the effect of linearization, are controlled by *separate contributions*. These quantities, which we require to be computable *a posteriori*, can potentially be exploited for the purpose of adaptively and interactively dealing with the respective approximation aspects.

With the aim of designing an adaptive numerical procedure for (1.1), we follow our recent work on stationary (elliptic) partial differential equations (PDEs) in Amrein & Wihler (2015), Amrein *et al.* (2016), Amrein & Wihler (2016) (see also Deuflhard, 2004; El Alaoui *et al.*, 2011). In particular, this includes the application of a Newton linearization framework to the nonlinear problem at hand, and, subsequently, the discretization of the resulting *sequence of linear evolution problems* by appropriate numerical schemes. It is worth mentioning that this methodology enables the use of numerical analysis techniques that originate from the treatment of *linear* problems; this is opposed to studying nonlinear discretization schemes (see, e.g., Kyza & Makridakis, 2011; Cangiani *et al.*, 2015). The challenge in deriving practically effective *a posteriori* error bounds within this setting is to provide a suitable splitting of the total residual into several computable quantities, each of which accounts for one of the different errors that have been committed during the discretization process: (R1) a linearization residual, (R2) a time discretization residual, and (R3) a space discretization residual. Then, based on the resulting *a posteriori* error estimates, a fully adaptive Newton–Galerkin time-stepping algorithm for the numerical solution of (1.1) can be derived. Specifically, in order to obtain an efficient overall complexity of the scheme, we propose an *interplay* between the Newton linearization, time adaptivity and spatial adaptivity. To do so, the algorithm will take into account the different residuals (R1)–(R3), and will perform a Newton step, a refinement of the current time step, or a refinement of the spatial mesh according to whichever residual is currently dominant.

In the context of this article, a $\mathbb{P}_1$-finite element approach in space, and a backward Euler discretization in time will be applied. Our *a posteriori* error analysis proceeds along the lines of the theory presented in Verfürth (2013) on linear parabolic equations. Furthermore, in order to obtain ε-robust bounds, we will follow the papers by Verfürth (1998) and Amrein & Wihler (2015) on finite element discretizations for singularly perturbed linear and semilinear elliptic problems, respectively. By means of a series of numerical experiments, we will demonstrate that the interactive application of temporal and spatial mesh refinements, together with a continued monitoring of the linearization effect, leads to an ε-robust control of the residual even in the singularly perturbed regime.

Outline. The article is organized as follows. In Section 2, we begin by deriving the Newton linearization of (1.1), and formulate the discretization of the resulting sequence of linearized problems in the spatial and temporal variables by means of a finite element method and the backward Euler scheme, respectively. Furthermore, the goal of Section 3 is to derive an ε-robust *a posteriori* error analysis. Moreover, in Section 5, we develop a fully adaptive Newton–Galerkin time-stepping algorithm. Furthermore, we present a series of numerical experiments illustrating the performance of the proposed adaptive procedure. Finally, we summarize our findings in Section 6.

Notation and problem formulation. For the purpose of this article, we define the space $V := H^1_0(\Omega)$, where $H^1_0(\Omega)$ is the standard Sobolev space of functions in $H^1(\Omega) = W^{1,2}(\Omega)$, with zero trace on $\partial\Omega$. The space V is equipped with the singular perturbation norm $\|\cdot\|_V := |||\cdot|||_{\varepsilon,\Omega}$, where, for any subset $D \subseteq \Omega$, we define

$$|||u|||_{\varepsilon,D} := \left(\varepsilon \, \|\nabla u\|^2_{0,D} + \|u\|^2_{0,D}\right)^{1/2}, \qquad u \in H^1(D).$$

Here, $\|\cdot\|_{0,D}$ denotes the L^2-norm on D. Frequently, for $D = \Omega$, the subindex 'D' will be omitted. In the sequel, we will abbreviate $f(u, \boldsymbol{x}, t)$ by $f(u)$, thereby suppressing the explicit dependence of f on the space and time variables; note that, in the case of $f(u) = -u$, when (1.1) is linear, the norm $|||\cdot|||_{\varepsilon,\Omega}$ is the natural energy norm on V.

Moreover, we signify by $V' = H^{-1}(\Omega)$ the dual space of V; it is equipped with the norm

$$\|\psi\|_{V'} := \sup_{\substack{z\in V\\ \|z\|_V=1}} \langle \psi, z\rangle,$$

where $\langle\cdot,\cdot\rangle$ is the dual product in $V' \times V$. Furthermore, consider the Bochner spaces $Y_T := L^2(0,T;V')$, and $X_T := \{u \in L^2(0,T;V) : \partial_t u \in Y_T\}$, with ∂_t being the time derivative operator in the distributional sense. For given $u \in X_T$ and $t \in (0,T)$, we have $u(t) = u(\cdot,t) \in V$. Then, defining the map $\mathsf{F}_\varepsilon : X_T \to Y_T$ through

$$\langle \mathsf{F}_\varepsilon(u(t)), v\rangle := \langle \partial_t u(t), v\rangle + \int_\Omega \{\varepsilon \nabla u(t)\cdot\nabla v - f(u(t))v\}\,\mathrm{d}\boldsymbol{x} \qquad \forall\, v \in V,\ t \in (0,T), \tag{1.2}$$

problem (1.1) can be written as a nonlinear operator equation in Y_T:

$$u \in X_T : \qquad \mathsf{F}_\varepsilon(u) = 0, \tag{1.3}$$

with $u(\cdot,0) = g$. We emphasize that formulation (1.3) is *strong* in time in the sense that it is based on testing (1.1) with time-independent functions in V; this is in contrast to *weak* space-time formulations of (1.1), in which test functions depend on both space and time (and in which integration is done with respect to both variables); cf., e.g., Roubíček (2005, Sect. 8.1).

Throughout this work, we shall use the abbreviation $x \preccurlyeq y$ to mean $x \le cy$, for a constant $c > 0$ depending neither on the space and time discretization parameters nor on $\varepsilon > 0$.

2. Linearization and discretization

2.1 *Linearization*

For given $u, w \in X_T$, and $t \in (0,T)$, we note that the Fréchet derivative of F_ε from (1.2) is given by

$$\left\langle \mathsf{F}'_\varepsilon(u(t))w(t), v\right\rangle = \langle \partial_t w(t), v\rangle + \int_\Omega \{\varepsilon\nabla w(t)\cdot\nabla v - \partial_u f(u(t))w(t)v\}\,\mathrm{d}\boldsymbol{x} \qquad \forall\, v \in V,\ t \in (0,T),$$

and is well defined provided that $\partial_u f(u) \in L^\beta(\Omega)$ for all $t \in (0,T)$, with $\beta \ge 1$ for $d = 1$ and $\beta > 1$ for $d = 2$; cf. Amrein & Wihler (2015, Lemma A.1). Then, starting from an initial guess $u_0 \in X_T$, Newton's method for (1.1) is an iterative procedure by which we find $u_{N+1} \in X_T$ from $u_N \in X_T$, for $N = 0, 1, 2\ldots$, such that there holds

$$\mathsf{F}'_\varepsilon(u_N)(u_{N+1} - u_N) = -\mathsf{F}_\varepsilon(u_N) \tag{2.1}$$

in Y_T. Upon defining the increment $\delta_N := u_{N+1} - u_N \in X_T$, and recalling (1.2), we note that

$$\langle \partial_t(u_N + \delta_N), v\rangle + \int_\Omega \{\varepsilon\nabla(u_N + \delta_N)\cdot\nabla v\}\,\mathrm{d}\boldsymbol{x} = \int_\Omega \{f(u_N) + \partial_u f(u_N)\delta_N\}v\,\mathrm{d}\boldsymbol{x}, \tag{2.2}$$

for all $v \in V$.

2.2 *Finite element meshes and spaces*

Let $\mathscr{T}_h = \{K\}_{K\in\mathscr{T}_h}$ be a regular and shape-regular mesh partition of Ω into disjoint open simplices, i.e., any $K \in \mathscr{T}_h$ is an affine and nondegenerate image of the (open) reference simplex $\widehat{K} = \{\widehat{x} \in \mathbb{R}^d_+ : \sum_{i=1}^d \widehat{x}_i < 1\}$. By $h_K = \operatorname{diam}(K)$, we signify the element diameter of $K \in \mathscr{T}_h$, and by $h = \max_{K\in\mathscr{T}_h} h_K$ the mesh size of $\mathscr{T}_h$. Furthermore, by $\mathscr{E}_h$ we denote the set of all interior mesh nodes for $d = 1$ and interior (open) edges for $d = 2$ in $\mathscr{T}_h$. In addition, for $K \in \mathscr{T}_h$, we let $\mathscr{E}_h(K) = \{E \in \mathscr{E}_h : E \subset \partial K\}$. For $E \in \mathscr{E}_h$, we let h_E be the mean of the lengths of the adjacent elements in one dimension, and the length of E in two dimensions.

We consider the finite element space of continuous, piecewise linear functions on $\mathscr{T}_h$ with zero trace on $\partial\Omega$, given by

$$V_0^h := \{\varphi \in H_0^1(\Omega) : \varphi|_K \in \mathbb{P}_1(K)\,\forall K \in \mathscr{T}_h\},$$

where $\mathbb{P}_1(K)$ is the standard space of all linear polynomial functions on K. Moreover, for any function $\varphi \in V_0^h$ and a given edge $E \in \mathscr{E}_h$ with $E = \mathscr{E}_h(K^\sharp)\cap\mathscr{E}_h(K^\flat)$ shared by two neighbouring simplices $K^\sharp, K^\flat \in \mathscr{T}_h$, we denote by $[\![\varphi]\!]_E$ the (vector-valued) jump of φ across E:

$$[\![\varphi]\!]_E(x) = \lim_{t\to 0^+} \varphi(\boldsymbol{x} + t\boldsymbol{n}^\sharp)\boldsymbol{n}^\sharp + \lim_{t\to 0^+} \varphi(\boldsymbol{x} + t\boldsymbol{n}^\flat)\boldsymbol{n}^\flat \qquad \forall\, \boldsymbol{x} \in E.$$

Here, $\boldsymbol{n}^\sharp$ and $\boldsymbol{n}^\flat$ denote the unit outward vectors on $\partial K^\sharp$ and $\partial K^\flat$, respectively. Furthermore, for any $K \in \mathscr{T}_h$, we consider the element patch

$$\omega_K := \bigcup_{\substack{K'\in\mathscr{T}_h:\\ \overline{K}\cap\overline{K}'\neq\emptyset}} K'.$$

2.3 *Newton–Galerkin backward Euler discretization*

In order to provide a numerical approximation of (1.1), we will discretize the spatial and temporal variables in formulation (2.1) by means of a finite element method in space and the backward Euler scheme in time, respectively. In combination with the Newton iteration this results in a Newton–Galerkin time-stepping approximation scheme.

We therefore consider a time partition of the interval $(0, T)$ into $M \geq 1$ subintervals $I_n = (t_{n-1}, t_n)$, $n = 1, \ldots, M$, satisfying $0 = t_0 < t_1 < \cdots < t_{M-1} < t_M = T$, and define the time-step lengths $k_n := t_n - t_{n-1}$. We mark any quantities related to the finite element discretization on a given time interval I_n by an index 'n'; in particular, we denote by $\mathscr{T}_h^n$ the corresponding spatial partition of Ω, and by

$$V_0^{h,n} := \{\varphi \in H_0^1(\Omega) : \varphi|_K \in \mathbb{P}_1(K)\,\forall K \in \mathscr{T}_h^n\}$$

the associated finite element space on a time subinterval I_n. Furthermore, for $n = 1, \ldots, M$, we signify by $\Pi^n : L^2(\Omega) \to V_0^{h,n}$ the L^2-projection onto $V_0^{h,n}$.

Applying the backward Euler time-stepping scheme, the finite element discretization of the Newton iteration (2.2) on each time interval I_n, $n = 1, 2, \ldots, M$ is to find $\delta_N^n \in V_0^{h,n}$ from $u_N^n \in V_0^{h,n}$ such that

$$\int_\Omega \left\{ \frac{u_N^n + \delta_N^n - u^{n-1}}{k_n} v + \varepsilon\nabla(u_N^n + \delta_N^n)\cdot\nabla v \right\} \mathrm{d}\boldsymbol{x} = \int_\Omega \left\{ f^n(u_N^n) + \partial_u f^n(u_N^n)\delta_N^n \right\} v \,\mathrm{d}\boldsymbol{x} \qquad \forall\, v \in V_0^{h,n}, \tag{2.3}$$

with the update $u_{N+1}^n = u_N^n + \delta_N^n$, and with

$$f^n(\cdot) := f(u, \boldsymbol{x}, t)|_{(\cdot, \boldsymbol{x}, t_n)}, \qquad \partial_u f^n(\cdot) := \partial_u f(u, \boldsymbol{x}, t)|_{(\cdot, \boldsymbol{x}, t_n)}.$$

Moreover, for $n = 2, \ldots, M$, we denote by $u^{n-1} \in V_0^{h,n-1}$ the (space-dependent) discrete solution at the previous time node t_{n-1} (resulting from a sufficient number of Newton iterations), and for $n = 1$, we let $u^0 := \pi^0 g \in V$ be an approximation of g if $g \notin V$. Furthermore, for the nth time step, the initial guess $u_0^n \in V_0^{h,n}$ is defined by

$$u_0^n := \Pi^n u^{n-1}, \quad 1 \le n \le M. \tag{2.4}$$

We will denote the procedure of performing one Newton update, i.e., solving (2.3) to obtain u_{N+1}^n, by

$$u_{N+1}^n = \texttt{solve}(k_n, \mathscr{T}_h^n, u_N^n).$$

Here, we make the assumption that we reinitiate the Newton iteration on each time step, i.e., for each $n = 1, 2, \ldots, M$, we start with the counter $N = 0$. For simplicity, we assume that the integrals on the right-hand side of (2.3) are evaluated exactly.

REMARK 2.1 The adaptive procedure based on the *a posteriori* analysis to be presented in the next sections enables the use of possible coarsening of some (spatial) elements with small error contributions. A coarsening strategy within the procedure of solving (2.3) is not a trivial task. In fact, suppose we have solved (2.3) up to time t_{n-1} so that we are given $u^{n-1} \in V_0^{h,n-1}$. Then, for a time step $k_n > 0$ small enough, it is reasonable to assume that u^{n-1} is located in an attracting γ-ball $B_\gamma(u_\infty^n) \subset \mathscr{A}(u_\infty^n)$, $\gamma > 0$, of $u_\infty^n \in V_0^{h,n}$, where $\mathscr{A}(u_\infty^n)$ denotes the attractor of the Newton iteration corresponding to u_∞^n. Thence, we have

$$\left\|u_0^n - u_\infty^n\right\| \le \left\|\Pi^n u^{n-1} - u^{n-1}\right\| + \left\|u^{n-1} - u_\infty^n\right\| \le \left\|\Pi^n u^{n-1} - u^{n-1}\right\| + \gamma, \tag{2.5}$$

for some suitable norm $\|\cdot\|$. Hence, if $\mathscr{T}_h^n$ is obtained from $\mathscr{T}_h^{n-1}$ by refinement only, then we see from (2.5) that $u_0^n \in \mathscr{A}(u_\infty^n)$ since $\Pi^n u^{n-1} = u^{n-1}$. If, however, coarsening is involved, then we usually have $\Pi^n u^{n-1} \neq u^{n-1}$, and in consequence, the quantity $\left\|\Pi^n u^{n-1} - u^{n-1}\right\|$ in (2.5) may be too large in order to guarantee that u_0^n stays within $\mathscr{A}(u_\infty^n)$. Thus any coarsening strategy should remove only those degrees of freedom for which $\left\|\Pi^n u^{n-1} - u^{n-1}\right\|$ remains of moderate size; cf. also Cangiani *et al.* (2015). In computing practice, the stability of the Newton iteration with respect to coarsening (i.e., the magnitude of $\left\|\Pi^n u^{n-1} - u^{n-1}\right\|$) is expected to depend strongly on the nonlinearity f (i.e., on the structure of the attractors) as well as on the initial guess for the Newton steps.

3. *A posteriori error analysis*

The goal of this section is to derive a residual-based *a posteriori* error bound for the discretization scheme (2.3), which can be employed for the purpose of formulating an adaptive refinement procedure for the meshes and time steps in each Newton step. This leads to a fully adaptive Newton–Galerkin backward Euler discretization method for (1.1). In the subsequent *a posteriori* error analysis, we follow closely the approach presented in Verfürth (2013).

3.1 *Residuals*

The discrete problem (2.3) generates a sequence $\{u_N^n\}_{N\geq 0}$ for each time step $n = 1, \ldots, M$. We can thus define a function $u_{\mathscr{I}} : [0, T] \to V$, time step by time step, by

$$u_{\mathscr{I}}(t) := \frac{t_n - t}{k_n} u^{n-1} + \frac{t - t_{n-1}}{k_n} u_{N+1}^n, \qquad t \in [t_{n-1}, t_n].$$

We emphasize that $u_{\mathscr{I}} \in C^0([0, T]; H_0^1(\Omega))$, with

$$u_{\mathscr{I}}(0) = \pi^0 g \in V. \tag{3.1}$$

Furthermore, we remark that $u_{\mathscr{I}}$ is understood as a function in time that depends on the (varying) Newton iteration counter N on each subinterval I_n. For later purposes notice that

$$q_n(t)\left(u^{n-1} - u_{N+1}^n\right) = u_{\mathscr{I}}(t) - u_{N+1}^n, \qquad t \in [t_{n-1}, t_n], \tag{3.2}$$

where $q_n(t) := k_n^{-1}(t_n - t)$, and, moreover, we observe that $\partial_t u_{\mathscr{I}} = k_n^{-1}(u_{N+1}^n - u^{n-1})$ on I_n, for $n = 1, \ldots, M$. Therefore, motivated by the linear case discussed in Verfürth (2013), we decompose the residual $\mathsf{F}_\varepsilon(u_{\mathscr{I}})$ from (1.2) on each time interval I_n, $n = 1, \ldots, M$ as

$$\langle \mathsf{F}_\varepsilon(u_{\mathscr{I}}), v\rangle = \left\langle \mathsf{F}_\varepsilon^1(u_{\mathscr{I}}), v\right\rangle + \left\langle \mathsf{F}_\varepsilon^2(u_{\mathscr{I}}), v\right\rangle + \left\langle \mathsf{F}_\varepsilon^3(u_{\mathscr{I}}), v\right\rangle, \qquad v \in V. \tag{3.3}$$

Here, on each time interval I_n, $n = 1, \ldots, M$, the parts $\mathsf{F}_\varepsilon^i(u_{\mathscr{I}})$, $i = 1, 2, 3$ are defined by

$$\begin{aligned}
\left\langle \mathsf{F}_\varepsilon^1(u_{\mathscr{I}}), v\right\rangle &:= \int_\Omega \{\partial_t u_{\mathscr{I}} v + \varepsilon \nabla u_{N+1}^n \cdot \nabla v - (f^n(u_N^n) + \partial_u f^n(u_N^n)\delta_N^n)v\}\,\mathrm{d}\boldsymbol{x},\\
\left\langle \mathsf{F}_\varepsilon^2(u_{\mathscr{I}}), v\right\rangle &:= \int_\Omega \varepsilon \nabla(u_{\mathscr{I}} - u_{N+1}^n) \cdot \nabla v\,\mathrm{d}\boldsymbol{x} + \int_\Omega \{f^n(u_{N+1}^n) - f(u_{\mathscr{I}})\}v\,\mathrm{d}\boldsymbol{x},\\
\left\langle \mathsf{F}_\varepsilon^3(u_{\mathscr{I}}), v\right\rangle &:= \int_\Omega \{f^n(u_N^n) + \partial_u f^n(u_N^n)\delta_N^n - f^n(u_{N+1}^n)\}v\,\mathrm{d}\boldsymbol{x},
\end{aligned}$$

for any $v \in V$. In accordance with the notation introduced in Verfürth (2013), we call $\mathsf{F}_\varepsilon^1(u_{\mathscr{I}})$ and $\mathsf{F}_\varepsilon^2(u_{\mathscr{I}})$ the *spatial* and the *temporal residuals*, respectively; furthermore, $\mathsf{F}_\varepsilon^3(u_{\mathscr{I}})$ is termed the *linearization residual*.

In view of an effective adaptive algorithm that is able to appropriately identify the individual error contributions resulting from the time and space discretizations as well as from the Newton linearization, it is of utmost importance how the residual $\mathsf{F}_\varepsilon(u_{\mathscr{I}})$ is split up. Specifically, the above residual decomposition (3.3) is based on three key points. First, the spatial residual is defined so that it tends to 0 for $h \to 0$. Second, we observe that the temporal residual also tends to 0 whenever $t_n \to t_{n-1}$, i.e., $u_{N+1}^n \to u^{n-1}$ (see also Verfürth, 2013, Sect. 6.1.4 in the case that (1.1) is linear). Third, the linearization residual features the crucial property that it converges to 0 for $u_{N+1}^n \to u_N^n$, i.e., when the Newton iteration converges.

3.2 *A posteriori error bound*

Upon applying the triangle inequality to the decomposition (3.3) we obtain

$$\|\mathsf{F}_\varepsilon(u_{\mathscr{I}})\|_{L^2(I_n;V')} \leq \left\|\mathsf{F}_\varepsilon^1(u_{\mathscr{I}})\right\|_{L^2(I_n;V')} + \left\|\mathsf{F}_\varepsilon^2(u_{\mathscr{I}})\right\|_{L^2(I_n;V')} + \left\|\mathsf{F}_\varepsilon^3(u_{\mathscr{I}})\right\|_{L^2(I_n;V')}, \tag{3.4}$$

on each time interval I_n, $n = 1, \dots, M$. We will now derive individual error bounds for each of the three residual terms $\mathsf{F}^i_\varepsilon(u_\mathscr{F})$, $i = 1, 2, 3$.

Spatial residual. We note the fact that the spatial residual $\mathsf{F}^1_\varepsilon(u_\mathscr{F})$ is constant with respect to time on each time interval I_n, $n = 1, \dots, M$. It can thus be estimated as in the stationary case (Amrein & Wihler, 2015, Theorem 4.4). In fact, observing that $\left\|\mathsf{F}^1_\varepsilon(u_\mathscr{F})\right\|_{L^2(I_n;V')} = \sqrt{k_n}\|\mathsf{F}^1_\varepsilon(u_\mathscr{F})\|_{V'}$, we infer the estimate

$$\left\|\mathsf{F}^1_\varepsilon(u_\mathscr{F})\right\|^2_{L^2(I_n;V')} \preccurlyeq k_n \sum_{K\in\mathscr{T}_h^n} \eta^2_{n,K,N}, \tag{3.5}$$

for any time interval I_n, $n = 1, \dots, M$. Here, for any $K \in \mathscr{T}_h^n$, the quantities

$$\eta^2_{n,K,N} := \alpha_K^2 \left\|f^n(u_N^n) + \partial_u f^n(u_N^n)\delta_N^n + \varepsilon\Delta u_{N+1}^n - \partial_t u_\mathscr{F}\right\|^2_{0,K} + \frac{1}{2}\sum_{E\in\mathscr{E}_h^n(K)} \varepsilon^{-1/2}\alpha_E \left\|\varepsilon[\![\nabla u_{N+1}^n]\!]\right\|^2_{0,E} \tag{3.6}$$

are computable residual indicators, where we define $\alpha_K := \min(1, \varepsilon^{-1/2}h_K)$ for $K \in \mathscr{T}_h$, and $\alpha_E := \min(1, \varepsilon^{-1/2}h_E)$ for $E \in \mathscr{E}_h$. We emphasize that the bound (3.5) is robust with respect to the singular perturbation parameter ε (as $\varepsilon \to 0$).

Temporal residual. Using the identity (3.2) we have

$$\left\langle \mathsf{F}^2_\varepsilon(u_\mathscr{F}), v\right\rangle = q_n \int_\Omega \{\varepsilon\nabla(u^{n-1} - u_{N+1}^n)\cdot\nabla v\}\,\mathrm{d}\boldsymbol{x} + \int_\Omega \{f^n(u_{N+1}^n) - f(u_\mathscr{F})\}v\,\mathrm{d}\boldsymbol{x},$$

on each time interval I_n, $n = 1, \dots, M$. Therefore, by application of the Cauchy–Schwarz inequality, we obtain

$$\|\mathsf{F}^2_\varepsilon(u_\mathscr{F})\|^2_{V'} \le q_n^2\varepsilon\|\nabla(u^{n-1} - u_{N+1}^n)\|_0^2 + \left\|f^n(u_{N+1}^n) - f(u_\mathscr{F})\right\|_0^2,$$

on I_n. Moreover, since $\int_{t_{n-1}}^{t_n} q_n(t)^2\,\mathrm{d}t = \frac{k_n}{3}$, we arrive at the bound

$$\left\|\mathsf{F}^2_\varepsilon(u_\mathscr{F})\right\|^2_{L^2(I_n;V')} \le k_n \sum_{K\in\mathscr{T}_h^n} \vartheta^2_{n,K,N}, \tag{3.7}$$

on each time interval I_n, $n = 1, \dots, M$, where we introduce the temporal residual indicator

$$\vartheta^2_{n,K,N} := k_n^{-1}\left\|f^n(u_{N+1}^n) - f(u_\mathscr{F})\right\|^2_{L^2(I_n;L^2(K))} + \tfrac{1}{3}\varepsilon\|\nabla(u^{n-1} - u_{N+1}^n)\|^2_{0,K}, \tag{3.8}$$

for $K \in \mathscr{T}_h^n$.

REMARK 3.1 Provided that $\left\|f^n(u^n_{N+1}) - f(u_{\mathscr{I}})\right\|^2_{L^2(\Omega))}$ is sufficiently smooth on I_n, then applying the trapezoidal rule we see that we have the approximation

$$\left\|f^n(u^n_{N+1}) - f(u_{\mathscr{I}})\right\|^2_{L^2(I_n;L^2(\Omega))} \approx \frac{k_n}{2}\left\|f^n(u^n_{N+1}) - f^{n-1}(u^{n-1})\right\|^2_0,$$

up to an error of order $\mathcal{O}(k_n^3)$, for each time interval I_n, $n = 1, \ldots, M$.

Linearization residual. We immediately infer

$$\|\mathsf{F}^3_\varepsilon(u_{\mathscr{I}})\|_{V'} \leq \left\|f^n(u^n_N) + \partial_u f^n(u^n_N)\delta^n_N - f^n(u^n_{N+1})\right\|_0,$$

and hence,

$$\left\|\mathsf{F}^3_\varepsilon(u_{\mathscr{I}})\right\|^2_{L^2(I_n;V')} \leq k_n \sum_{K\in\mathscr{T}^n_h} \Upsilon^2_{n,K,N}, \tag{3.9}$$

on each time step I_n, $n = 1, \ldots, M$, where we define the linearization residual indicator

$$\Upsilon_{n,K,N} := \left\|f^n(u^n_N) + \partial_u f^n(u^n_N)\delta^n_N - f^n(u^n_{N+1})\right\|_{0,K}, \qquad K \in \mathscr{T}^n_h. \tag{3.10}$$

Combining the bounds (3.4), (3.5), (3.7) and (3.9), leads to the following result.

THEOREM 3.2 On each time interval I_n, $n = 1, 2, \ldots, M$, there holds the *a posteriori* error bound

$$\|\mathsf{F}_\varepsilon(u_{\mathscr{I}})\|^2_{L^2(I_n;V')} \preccurlyeq k_n \sum_{K\in\mathscr{T}^n_h} \left\{\eta^2_{n,K,N} + \vartheta^2_{n,K,N} + \Upsilon^2_{n,K,N}\right\},$$

where, for $K \in \mathscr{T}^n_h$, we recall the spatial, temporal and linearization residual indicators from (3.6), (3.8) and (3.10), respectively.

For later reference, in addition to the previously introduced local *a posteriori* quantities, we define the corresponding global residual indicators as follows:

$$\eta^2_{n,\Omega,N} := \sum_{K\in\mathscr{T}^n_h} \eta^2_{n,K,N}, \qquad \vartheta^2_{n,\Omega,N} := \sum_{K\in\mathscr{T}^n_h} \vartheta^2_{n,K,N}, \qquad \Upsilon^2_{n,\Omega,N} := \sum_{K\in\mathscr{T}^n_h} \Upsilon^2_{n,K,N}. \tag{3.11}$$

3.3 *Residual and error norm*

Under certain conditions on the nonlinearity f in (1.1), it can be shown that the residual $\mathsf{F}_\varepsilon(u_{\mathscr{I}})$ defined in (1.2) and the error $u - u_{\mathscr{I}}$ are equivalent. For example, suppose that the nonlinearity f is Lipschitz continuous with Lipschitz constant $L > 0$, i.e.,

$$|f(u, \boldsymbol{x}, t) - f(v, \boldsymbol{x}, t)| \leq L|u - v|,$$

and that it satisfies the monotonicity condition

$$(f(u,\boldsymbol{x},t)-f(v,\boldsymbol{x},t))(u-v)\leq 0$$

for all $u,v\in\mathbb{R},\boldsymbol{x}\in\Omega,t\in[0,T]$. Then, if u is the exact solution of (1.3), we have

$$\begin{aligned}-\langle \mathsf{F}_\varepsilon(u_\mathscr{f}),u-u_\mathscr{f}\rangle &= \frac{1}{2}\frac{\mathrm{d}}{\mathrm{d}t}\|u-u_\mathscr{f}\|_0^2+\varepsilon\|\nabla(u-u_\mathscr{f})\|_0^2-\int_\Omega (f(u)-f(u_\mathscr{f}))(u-u_\mathscr{f})\,\mathrm{d}\boldsymbol{x}\\ &\geq \frac{1}{2}\frac{\mathrm{d}}{\mathrm{d}t}\|u-u_\mathscr{f}\|_0^2+\varepsilon\|\nabla(u-u_\mathscr{f})\|_0^2\end{aligned}$$

for any $t\in(0,T)$. Proceeding as in Amrein & Wihler (2015, Eq. (4.13)) it holds that

$$-\langle \mathsf{F}_\varepsilon(u_\mathscr{f}),u-u_\mathscr{f}\rangle\geq\frac{1}{2}\frac{\mathrm{d}}{\mathrm{d}t}\|u-u_\mathscr{f}\|_0^2+C_\varepsilon|\!|\!|u-u_\mathscr{f}|\!|\!|_\varepsilon^2,$$

where $C_\varepsilon=(1+\varepsilon^{-1}c_\Omega)^{-1}$, with a constant $c_\Omega>0$ depending only on Ω. Furthermore, choosing $\delta>0$ such that $C_{\delta,\varepsilon}:=C_\varepsilon-\delta/2>0$, and using

$$|\langle \mathsf{F}_\varepsilon(u_\mathscr{f}),u-u_\mathscr{f}\rangle|\leq\frac{1}{2}\left(\delta^{-1}\|\mathsf{F}_\varepsilon(u_\mathscr{f})\|_{V'}^2+\delta|\!|\!|u-u_\mathscr{f}|\!|\!|_\varepsilon^2\right),$$

we conclude

$$\frac{1}{2}\frac{\mathrm{d}}{\mathrm{d}t}\|u-u_\mathscr{f}\|_0^2+C_{\delta,\varepsilon}|\!|\!|u-u_\mathscr{f}|\!|\!|_\varepsilon^2\leq\frac{1}{2\delta}\|\mathsf{F}_\varepsilon(u_\mathscr{f})\|_{V'}^2.\tag{3.12}$$

Integrating with respect to t and exploiting (3.1) yields

$$\int_0^t|\!|\!|u-u_\mathscr{f}|\!|\!|_\varepsilon^2\,\mathrm{d}t\leq\frac{\max\{1,\delta^{-1}\}}{2C_{\delta,\varepsilon}}\left(\|\mathsf{F}_\varepsilon(u_\mathscr{f})\|_{L^2(0,t;V')}^2+\left\|g-\pi^0 g\right\|_0^2\right).\tag{3.13}$$

In addition, invoking again (3.12), we obtain

$$\|u-u_\mathscr{f}\|_{L^\infty(0,t;L^2(\Omega))}^2\leq\max\{1,\delta^{-1}\}\left(\|\mathsf{F}_\varepsilon(u_\mathscr{f})\|_{L^2(0,t;V')}^2+\left\|g-\pi^0 g\right\|_0^2\right).\tag{3.14}$$

Moreover, applying the Lipschitz continuity of f, we observe, for $v\in V$ and $t\in(0,T]$, that

$$|\langle\partial_t(u-u_\mathscr{f}),v\rangle|\leq|\langle \mathsf{F}_\varepsilon(u_\mathscr{f}),v\rangle|+\int_\Omega\{\varepsilon|\nabla(u-u_\mathscr{f})||\nabla v|+L|u-u_\mathscr{f}||v|\}\,\mathrm{d}\boldsymbol{x},$$

i.e., there holds

$$|\langle\partial_t(u-u_\mathscr{f}),v\rangle|\leq|\langle \mathsf{F}_\varepsilon(u_\mathscr{f}),v\rangle|+\max(1,L)|\!|\!|v|\!|\!|_\varepsilon|\!|\!|u-u_\mathscr{f}|\!|\!|_\varepsilon.$$

Thus, dividing by $|\!|\!|u-u_\mathscr{f}|\!|\!|_\varepsilon$, we deduce that

$$\|\partial_t(u-u_\mathscr{f})\|_{V'}\leq\|\mathsf{F}_\varepsilon(u_\mathscr{f})\|_{V'}+\max(1,L)|\!|\!|u-u_\mathscr{f}|\!|\!|_\varepsilon.\tag{3.15}$$

Taking the square in the previous inequality, integrating over $(0,t)$, and recalling (3.13) leads to

$$\|\partial_t(u-u_{\mathscr{I}})\|^2_{L^2(0,t;V')} \leq C_{\delta,\varepsilon,L}\left(\|\mathsf{F}_\varepsilon(u_{\mathscr{I}})\|^2_{L^2(0,t;V')} + \left\|g-\pi^0 g\right\|^2_0\right), \tag{3.16}$$

with

$$C_{\delta,\varepsilon,L} := 2 + \frac{\max(1,L^2)\max(1,\delta^{-1})}{C_{\delta,\varepsilon}}.$$

Combining (3.13), (3.14) and (3.16), we finally get

$$\begin{aligned} E(t;u_{\mathscr{I}},g) &:= \left\|g-\pi^0 g\right\|^2_0 + \|u-u_{\mathscr{I}}\|^2_{L^\infty(0,t;L^2(\Omega))} + \int_0^t \left\{|\!|\!| u-u_{\mathscr{I}} |\!|\!|^2_\varepsilon + \|\partial_t(u-u_{\mathscr{I}})\|^2_{V'}\right\} \mathrm{d}t \\ &\leq \widetilde{C}_{\delta,\varepsilon,L}\left(\|\mathsf{F}_\varepsilon(u_{\mathscr{I}})\|^2_{L^2(0,t;V')} + \left\|g-\pi^0 g\right\|^2_0\right), \end{aligned}$$

with

$$\widetilde{C}_{\delta,\varepsilon,L} := 3 + \max(1,\delta^{-1}) + \frac{3\max(1,\delta^{-1})\max(1,L^2)}{2C_{\delta,\varepsilon}},$$

and any $t \in (0,T]$. Conversely, proceeding as in (3.15), it is possible to show

$$\|\mathsf{F}_\varepsilon(u_{\mathscr{I}})\|_{V'} \leq \|\partial_t(u-u_{\mathscr{I}})\|_{V'} + \max(1,L)\,|\!|\!| u-u_{\mathscr{I}} |\!|\!|_\varepsilon .$$

Integrating over $(0,t)$ shows the equivalence of the residual term $\|\mathsf{F}_\varepsilon(u_{\mathscr{I}})\|_{L^2(0,t;V')} + \left\|g-\pi^0 g\right\|_0$ and the error expression $E(t;u_{\mathscr{I}},g)$.

4. A fully adaptive Newton–Galerkin algorithm

We will now propose a procedure that will combine a Newton method with automatic spatial finite element mesh and time-step refinements based on the *a posteriori* error estimate from Theorem 3.2. Recalling our derivations in the previous Section 3.3, it is reasonable to control the quantity

$$E^n(u_{\mathscr{I}},g) := \|\mathsf{F}_\varepsilon(u_{\mathscr{I}})\|^2_{L^2(0,t_n;V')} + \left\|g-\pi^0 g\right\|^2_0,$$

for $n = 1,\ldots,M$. Then, by means of Theorem 3.2, we have

$$E^n(u_{\mathscr{I}},g) \preccurlyeq \eta_0^2 + \sum_{j=1}^n k_j\left(\eta^2_{j,\Omega,N} + \vartheta^2_{j,\Omega,N} + \Upsilon^2_{j,\Omega,N}\right), \tag{4.1}$$

where $\eta_0 := \|g-\pi^0 g\|_0$ and $\eta_{j,\Omega,N}$, $\vartheta_{j,\Omega,N}$, and $\Upsilon_{j,\Omega,N}$ are defined in (3.11), for $1 \leq j \leq M$. Given a final time $T > 0$, and some positive tolerances $\varepsilon_0, \varepsilon_\eta, \varepsilon_\vartheta, \varepsilon_\Upsilon > 0$, we define

$$\varepsilon_{\mathrm{loc},\eta} := \varepsilon_\eta/\sqrt{T}, \quad \varepsilon_{\mathrm{loc},\vartheta} := \varepsilon_\vartheta/\sqrt{T}, \quad \varepsilon_{\mathrm{loc},\Upsilon} := \varepsilon_\Upsilon/\sqrt{T}. \tag{4.2}$$

Suppose

$$\eta_0 \leq \varepsilon_0, \tag{4.3}$$

and, for any $n = 1, \ldots, M$, there holds

$$\eta_{n,\Omega,N} \leq \varepsilon_{\mathrm{loc},\eta}, \quad \vartheta_{n,\Omega,N} \leq \varepsilon_{\mathrm{loc},\vartheta}, \quad \Upsilon_{n,\Omega,N} \leq \varepsilon_{\mathrm{loc},\Upsilon}.$$

Then, we conclude

$$E^M(u_{\mathscr{I}}, g) \preccurlyeq \varepsilon_T^2, \tag{4.4}$$

where $\varepsilon_T^2 := \varepsilon_0^2 + \varepsilon_\eta^2 + \varepsilon_\vartheta^2 + \varepsilon_\Upsilon^2$.

We now formulate a possible realization of a time-space-Newton–Galerkin adaptive algorithm which aims to generate a numerical solution $u_{\mathscr{I}}$ that satisfies the error bound (4.4). The basic idea is to exploit the structure of the error bound (4.1) to provide an *interplay* between adaptive finite element space refinements (and coarsenings), automatic selection of the time steps, and an appropriate resolution of the Newton linearization error. More precisely, our adaptive procedure identifies whichever of the computable *a posteriori* quantities occurring in (4.1) is currently dominant, and performs a corresponding refinement. In this way, the scheme follows the lines of our previous approach in Amrein *et al.* (2016) and Amrein & Wihler (2015, 2016) on stationary problems, with the additional feature that the temporal errors are now taken into account, too. Our fully adaptive Newton–Galerkin method is outlined in Algorithm 1.

REMARK 4.1 As already emphasized in Remark 2.1, step 6 in Algorithm 1 may be delicate to realize if coarsening of the spatial mesh is taken into account. Indeed, in step 5, any coarsening procedure should be moderate in order to prevent the Newton iteration from leaving the current basin of attraction.

We also remark that the parameter $k_{\min} > 0$ in step 4 guarantees that the step size k_n does not become overly small. This restriction needs to be relaxed when resolving *finite time blow-up problems*, where the adaptivity with respect to the time evolution requires arbitrarily small step sizes k_n close to the blow-up time; see, e.g., Bandle & Brunner (1998), Nakagawa (1975), Janssen & Wihler (2015) for details.

5. Numerical experiments

We will now illustrate and test Algorithm 1 by means of a number of numerical experiments. We choose the initial spatial meshes to be sufficiently fine (to fulfil (4.3)). Elements $K \in \mathscr{T}_h^n$ are coarsened whenever $\eta_{n,K,N} < 0.1\overline{\eta}_{n,\Omega,N}$, where $\overline{\eta}_{n,\Omega,N}$ signifies the mean of all $\eta_{n,K,N}$, $K \in \mathscr{T}_h^n$; see (3.6).

EXAMPLE 5.1 On $\Omega = (0,1)$ let us consider the *linear* singularly perturbed initial/boundary value problem

$$\begin{aligned} \partial_t u - \varepsilon \partial_{xx} u &= \exp(t) && \text{on } \Omega \times (0,T], \\ u &= 0 && \text{on } \{0,1\} \times (0,T], \\ u(0,\cdot) &= g_\varepsilon && \text{in } \Omega, \end{aligned} \tag{5.1}$$

Algorithm 1 Fully-adaptive Newton–Galerkin time-stepping method

1: Initialization: Input a final time $T > 0$. Prescribe the overall error $\varepsilon_T > 0$, a lower bound for the time steps $k_{\min} > 0$, an initial time step $k_0 \geq k_{\min}$ and two time mesh parameters $\kappa > 1$ (coarsening) and $\sigma \in (0,1)$ (refinement). Generate an initial mesh $\mathscr{T}_h^1$ in Ω. Set $n \leftarrow 1$.
2: Choose $\pi^0 g \in V$ such that $\varepsilon_0 := \|g - \pi^0 g\|_0 < \varepsilon_T$ (note that this is always possible by density of $V \subset L^2(\Omega)$).
3: Split the tolerance ε_T into contributions $\varepsilon_\eta, \varepsilon_\vartheta, \varepsilon_\Upsilon > 0$ such that there holds $\varepsilon_T^2 := \varepsilon_0^2 + \varepsilon_\eta^2 + \varepsilon_\vartheta^2 + \varepsilon_\Upsilon^2$.
4: **while** $k_n := \min\{k_{n-1}, T - t_{n-1}\} \geq k_{\min}$ **do** ▷ time stepping
5: On the current mesh $\mathscr{T}_h^n$ (nth time step), compute the initial guess u_0^n for the Newton iteration from (2.4); set $N \leftarrow 0$.
6: Compute $u_{N+1}^n = \texttt{solve}(k_n, \mathscr{T}_h^n, u_N^n)$, and evaluate the residual indicators from (3.6), (3.8) and (3.10).
7: **if** $\eta_{n,\Omega,N}^2 + \vartheta_{n,\Omega,N}^2 + \Upsilon_{n,\Omega,N}^2 > \varepsilon_{\mathrm{loc},\eta}^2 + \varepsilon_{\mathrm{loc},\vartheta}^2 + \varepsilon_{\mathrm{loc},\Upsilon}^2$ **then**
8: **if** $\vartheta_{n,\Omega,N}^2 + \Upsilon_{n,\Omega,N}^2 < \eta_{n,\Omega,N}^2$ **then**
9: Refine and coarsen the current mesh $\mathscr{T}_h^n$ according to the elemental contributions in order to obtain a new mesh $\mathscr{T}_h^n \leftarrow \mathscr{T}_h^n$; go back to step 5.
10: **else if** $\Upsilon_{n,\Omega,N} < \vartheta_{n,\Omega,N}$ **then**
11: Set $k_n \leftarrow \sigma k_n$, $N \leftarrow 0$ and go to step 5 (if $k_n \geq k_{\min}$, otherwise stop algorithm).
12: **else if** $\Upsilon_{n,\Omega,N} \geq \vartheta_{n,\Omega,N}$ **then**
13: Do another Newton iteration by going back to step 6.
14: **end if**
15: **else if** $t_{n-1} + k_n = T$ **then**
Stop the algorithm.
16: **else**
17: Let $k_n \leftarrow \kappa k_n$, and set $n \leftarrow n + 1$.
18: **end if**
19: **end while**

where g_ε is the solution of the elliptic boundary value problem $-\varepsilon g_\varepsilon'' + g_\varepsilon = 1$, with $g_\varepsilon(0) = g_\varepsilon(1) = 0$. Note that g_ε exhibits boundary layers at $x \in \{0,1\}$; cf. Amrein & Wihler (2015). Since the problem is linear, the Newton iteration is redundant in this example. We prescribe the time coarsening/refinement parameters $\kappa = 2, \sigma = 1/2$. Moreover, we compute a numerical solution up to the final time $T = 1$, and set the local error tolerances from (4.2) (as well as ε_0 given in (4.3)) to 10^{-3}. Furthermore, the initial time step k_0 is chosen to be $1/10$.

Our goal here is to test the robustness of the *a posteriori* error analysis with respect to ε as $\varepsilon \to 0$. To this end, we quantify the performance of our algorithm by comparing the true error

$$\|u - u_{\mathscr{I}}\|_{L^2(0,t_n;V)}^2 + \|u - u_{\mathscr{I}}\|_{L^\infty(0,t_n;L^2(\Omega))}^2$$

with the estimated error (i.e., the right-hand side of (4.1)), and compute the time-dependent efficiency indices (defined by the ratio of these quantities for $n \in \{1,2,\ldots,M\}$); the results are displayed in Fig. 1 for $\varepsilon = 10^{-p}$, with $p \in \{1,2,3,4,5\}$. They show that the boundary layers close to $\{0,1\}$ are properly resolved, and clearly highlight the robustness of the efficiency indices with respect to ε as $\varepsilon \to 0$.

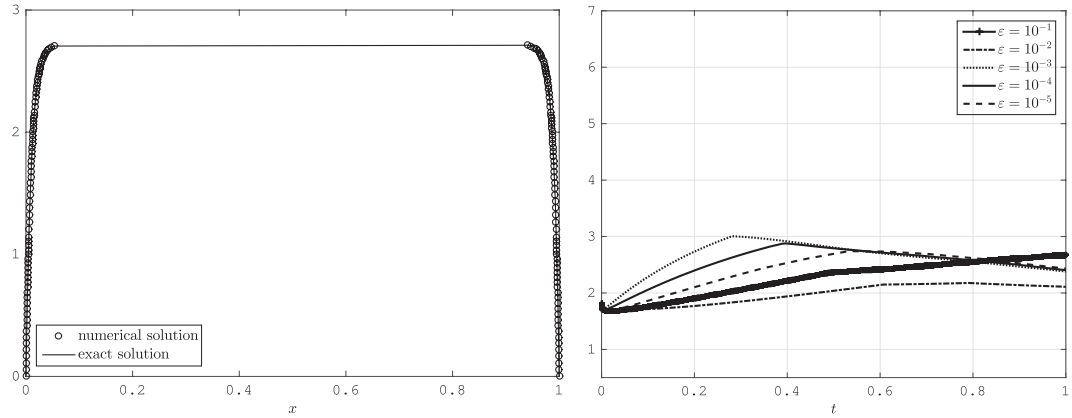

FIG. 1. Example 5.1: numerical solution (with '∘' indicating the mesh points) vs. exact solution at $T = 1$ (left), and (time-dependent) efficiency indices for various choices of ε (right).

EXAMPLE 5.2 Furthermore, on $\Omega = (0,1)$ consider the following nonlinear singularly perturbed initial/boundary value problem:

$$\begin{cases} \partial_t u - \varepsilon \partial_{xx} u = -u^4 + \sin(t) & \text{on } \Omega \times (0,T], \\ u = 0 & \text{on } \{0,1\} \times (0,T], \\ u(0,\cdot) = g & \text{in } \Omega. \end{cases} \tag{5.2}$$

Here we choose $g(x) := 1/2 \sin(\pi x)^2$. When evolving in time, problem (5.2) exhibits boundary layers for $0 < \varepsilon \ll 1$; see Fig. 2 (left), and Verhulst (2005) for a detailed discussion of this problem. We consider $\varepsilon = 10^{-5}$, and choose the local error tolerances from (4.2) (as well as ε_0 from (4.3)) to be 10^{-3}, and the initial time step as $k_0 = 1/4$. In Fig. 2 (right) we depict a log/log plot of the estimated error from (4.1) up to the final time $T = 2$. Notice that the slope $1/2$ in the log/log plot is due to the fact that

$$\sqrt{E^n(u_{\mathscr{I}}, g)} \preccurlyeq \left(\eta_0^2 + \sum_{l=1}^{n} k_l \left(\eta_{l,\Omega,N}^2 + \vartheta_{l,\Omega,N}^2 + \Upsilon_{l,\Omega,N}^2 \right) \right)^{1/2} \leq \left(\varepsilon_0^2 + t_n (\varepsilon_{\mathrm{loc},\eta}^2 + \varepsilon_{\mathrm{loc},\vartheta}^2 + \varepsilon_{\mathrm{loc},\Upsilon}^2) \right)^{1/2}$$

(cf. (4.1)), i.e., for sufficiently small $\varepsilon_0 > 0$, we expect the error to grow with order $\mathcal{O}(t_n^{1/2})$ as time evolves.

EXAMPLE 5.3 Finally, we consider the nonlinear problem

$$\begin{cases} \partial_t u - \varepsilon \partial_{xx} u = u^\beta & \text{on } \Omega \times (0,T], \\ u = 0 & \text{on } \{0,1\} \times (0,T], \\ u(0,\cdot) = g & \text{in } \Omega. \end{cases} \tag{5.3}$$

A detailed discussion of problems with power-type source terms can be found, for instance, in the monograph Samarskii *et al.* (1995). In particular, for $\beta > 1$, the solution of (5.3) will become unbounded

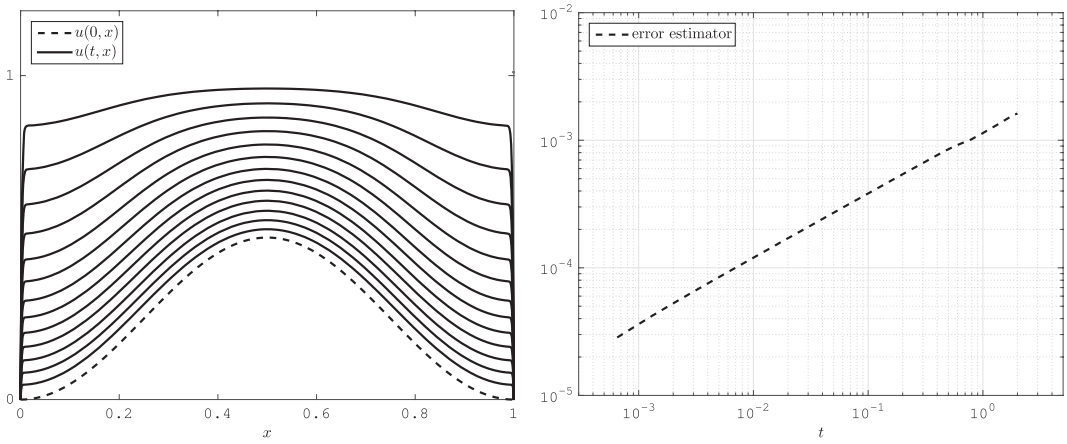

FIG. 2. Example 5.2: snapshots of the numerical solution (as time is evolving) corresponding to problem (5.2) with $\varepsilon = 10^{-5}$ (left), and the estimated error for $\sqrt{E^n(u_{\mathscr{J}}, g)}$ (right).

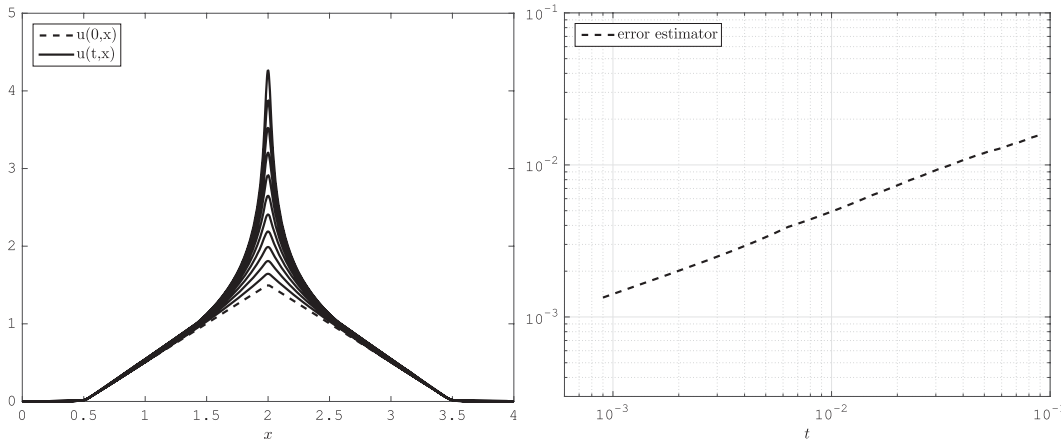

FIG. 3. Example 5.3: snapshots of the numerical solution (as time is evolving) corresponding to problem (5.3) with $\varepsilon = 10^{-3}$, $\beta = 4$, $\Omega = (0, 4)$ (left), and the estimated error for $\sqrt{E^n(u_{\mathscr{J}}, g)}$ (right).

in finite time provided that the initial data $u(0, \cdot) = g \geq 0$ is suitably chosen. In this example, g is piecewise linear with $g(2) = 3/2$ and support on $(1/2, 7/2)$.

On the left of Fig. 3, we show the numerical solution of (5.3) for $\Omega = (0, 4)$, $\beta = 4$, $\varepsilon = 10^{-3}$, and $T \approx 0.1$. The local error tolerances from (4.2) are set to 10^{-2}, and $k_0 = 10^{-3}$. On the right in Fig. 3, we present a log/log plot of the estimated error (i.e., the right-hand side of (4.1)) corresponding to the numerical solution shown on the left in Fig. 3. We clearly observe that the estimated error from (4.1) increases with slope $= 1/2$, as in Example 5.2. Moreover, as time evolves, we see that the adaptive procedure is able to resolve properly the spike located around $x = 2$.

6. Conclusions

The aim of this article is the development of a reliable and computationally efficient procedure for the numerical solution of semilinear parabolic boundary value problems with possible singular perturbations. The key idea is to exploit a suitable interplay between a local Newton linearization procedure (of the nonlinear PDE problem), of an automatic (spatial) finite element mesh refinement approach and of an adaptive time-stepping control process. The numerical scheme is studied within the context of a robust (with respect to the singular perturbations) residual-oriented *a posteriori* analysis, and a corresponding adaptive mesh refinement scheme is developed. Our numerical experiments clearly illustrate the ability of the proposed methodology to reliably find solutions, and to robustly resolve the singular perturbations at the expected rate. Important topics for future research include the use of anisotropic mesh refinements for two- and three-dimensional singularly perturbed problems, the development of suitable solvers and the application of higher-order time-stepping schemes.

Funding

The authors acknowledge the support of the Swiss National Science Foundation (SNF) Grant number 200021_162990.

References

Amrein, M., Melenk, J. M. & Wihler, T. P. (2016) An *hp*-adaptive Newton–Galerkin finite element procedure for semilinear boundary value problems. *Math. Methods Appl. Sci.* (to appear).

Amrein, M. & Wihler, T. P. (2015) Fully adaptive Newton–Galerkin methods for semilinear elliptic partial differential equations. *SIAM J. Sci. Comput.*, **37**, A1637–A1657.

Amrein, M. & Wihler, T. P. (2016) Adaptive pseudo transient-continuation-Galerkin methods for semilinear elliptic partial differential equations. *Technical Report*. Available at https://arxiv.org/abs/1607.01421, report arXiv:1607.01421.

Bandle, C. & Brunner, H. (1998) Blowup in diffusion equations: a survey. *J. Comput. Appl. Math.*, **97**, 3–22.

Barles, G. & Burdeau, J. (1995) The Dirichlet problem for semilinear second-order degenerate elliptic equations and applications to stochastic exit time control problems. *Commun. Partial Differ. Equ.*, **20**, 129–178.

Barles, G. & Perthame, B. (2007) Concentrations and constrained Hamilton–Jacobi equations arising in adaptive dynamics. *Recent Developments in Nonlinear Partial Differential Equations*. Contemporary Mathematics, vol. 439. Providence, RI: American Mathematical Society, pp. 57–68.

Borisyuk, A., Ermentrout, B., Friedman, A. & Terman, D. (2005) *Tutorials in Mathematical Biosciences. I*. Lecture Notes in Mathematics, vol. 1860. Mathematical Neuroscience, Mathematical Biosciences Subseries. Berlin: Springer.

Cangiani, A., Georgoulis, E. H., Kyza, I. & Metcalfe, S. (2015) Adaptivity and blow-up detection for nonlinear evolution problems. *Technical Report*. arXiv report 1502.03250.

Cantrell, R. S. & Cosner, C. (2003) *Spatial Ecology via Reaction-Diffusion Equations*. Wiley Series in Mathematical and Computational Biology. Chichester: Wiley.

Chandrasekhar, S. (1939) *An Introduction to the Study of Stellar Structure*. University of Chicago Press.

Deuflhard, P. (2004) Affine invariance and adaptive algorithms. *Newton Methods for Nonlinear Problems*. Springer Series in Computational Mathematics, vol. 35. Berlin: Springer.

Edelstein-Keshet, L. (2005) *Mathematical Models in Biology*. Classics in Applied Mathematics, vol. 46. Philadelphia, PA: Society for Industrial and Applied Mathematics (SIAM). Reprint of the 1988 original.

El Alaoui, L., Ern, A. & Vohralík, M. (2011) Guaranteed and robust a posteriori error estimates and balancing discretization and linearization errors for monotone nonlinear problems. *Comput. Methods Appl. Mech. Eng.*, **200**, 2782–2795.

JÄGER, W. & LUCKHAUS, S. (1992) On explosions of solutions to a system of partial differential equations modelling chemotaxis. *Trans. Am. Math. Soc.*, **329**, 819–824.

JANSSEN, B. & WIHLER, T. P. (2015) Continuous and discontinuous Galerkin time stepping methods for nonlinear initial value problems. *Technical Report*. Available at http://arxiv.org/abs/1407.5520.

KELLEY, P. L. (1965) Self-focusing of optical beams. *Phys. Rev. Lett.*, **15**, 1005–1008.

KYZA, I. & MAKRIDAKIS, C. (2011) Analysis for time discrete approximations of blow-up solutions of semilinear parabolic equations. *SIAM J. Numer. Anal.*, **49**, 405–426.

NAKAGAWA, T. (1975) Blowing up of a finite difference solution to $u_t = u_{xx} + u^2$. *Appl. Math. Optim. Int. J. Appl. Stoch.*, **2**, 337–350.

OKUBO, A. & LEVIN, S. A. (2001) *Diffusion and Ecological Problems: Modern Perspectives*, 2nd edn. Interdisciplinary Applied Mathematics, vol. 14. New York: Springer.

PERTHAME, B. (2007) *Transport Equations in Biology*. Frontiers in Mathematics. Basel: Birkhäuser.

ROOS, H.-G., STYNES, M. & TOBISKA, L. (2008) *Robust Numerical Methods for Singularly Perturbed Differential Equations*, 2nd edn. Springer Series in Computational Mathematics, vol. 24. Berlin: Springer.

ROUBÍČEK, T. (2005) *Nonlinear Partial Differential Equations with Applications*. International Series of Numerical Mathematics, vol. 153. Basel: Birkhäuser.

SAMARSKII, A., GALAKTIONOV, V., KURDYUMOV, S. & MIKHAILOV, A. (1995) *Blow-Up in Quasilinear Parabolic Equations*. De Gruyter Expositions in Mathematics, vol. 19. Berlin: Walter de Gruyter.

STUART, A. M. & FLOATER, M. S. (1990) On the computation of blow-up. *Eur. J. Appl. Math.*, **1**, 47–71.

VERFÜRTH, R. (1998) Robust a posteriori error estimators for a singularly perturbed reaction-diffusion equation. *Numer. Math.*, **78**, 479–493.

VERFÜRTH, R. (2013) *A Posteriori Error Estimation Techniques for Finite Element Methods*. Numerical Mathematics and Scientific Computation. Oxford: Oxford University Press, pp. xx+393.

VERHULST, F. (2005) *Methods and Applications of Singular Perturbations*. Texts in Applied Mathematics, vol. 50. New York: Springer.